

# PHYSICAL REVIEW LETTERS

VOLUME 57

25 AUGUST 1986

NUMBER 8

## New Universal Scenarios for the Onset of Chaos in Lorenz-Type Flows

Jean-Marc Gambaudo,<sup>(a)</sup> Itamar Procaccia, Stefan Thomae,<sup>(b)</sup> and Charles Tresser<sup>(c)</sup>

*Department of Chemical Physics, The Weizmann Institute of Science, Rehovot 76100, Israel*

(Received 24 February 1986)

It is shown that in simple three-dimensional flows there are uncountably many different codimension-2 scenarios for the onset of chaos. We analyze these scenarios via one-dimensional Poincaré maps, and show how to construct renormalization groups to obtain new universal results. Comparisons with numerical studies are given.

PACS numbers: 05.45.+b

The aim of this Letter is to stress that the variety of routes to chaos in even very simple flows is much wider than that seen in continuous maps of the interval.<sup>1</sup> The latter maps allowed us to study the three scenarios of period doubling, intermittency, and quasiperiodicity. In simple flows of the type of the Lorenz model<sup>2</sup> we find an infinity of routes to chaos reminiscent of the richness of complex analytic maps,<sup>3</sup> except that in our case we deal with the onset of chaos in generic cases. How these scenarios come about is explained here, and the example of period tripling is studied in some detail.

The basic reason for the greater richness of these flows is that their Poincaré sections can be reduced to maps of an interval<sup>4</sup>  $f: [-\mu, \nu] \rightarrow [-\mu, \nu]$ ,

$$f(x) = \begin{cases} f_L(x) = \nu - \alpha|x|^\zeta + \text{h.o.t.}, & x \leq 0, \\ f_R(x) = -\mu + bx^\zeta + \text{h.o.t.}, & x > 0, \end{cases} \quad (1)$$

$$\mu, \nu > 0, \quad \zeta > 1,$$

where "h.o.t." stands for "higher-order terms," and where  $f_L$  and  $f_R$  are increasing; see Fig. 1. With the condition  $f(-\mu) = f(\nu)$  one gets continuous circle maps, and with  $f(-x) \equiv -f(x)$  one gets maps equivalent<sup>5</sup> to one-hump maps  $g(x)$  where  $g(x) = f_L(x)$  for  $x \leq 0$ ,  $g(x) = -f_R(x)$  for  $x > 0$ . In general, however, these maps belong to a much larger space of functions and they exhibit richer dynamical behavior.<sup>6,7</sup>

To see how such maps come about consider a flow

in three dimensions which has the geometrical structure of the Lorenz flow<sup>4</sup> (see Fig. 2). Near the origin the flow reads  $(\dot{x}, \dot{y}, \dot{z}) = \eta_1 x, -\eta_3 y, -\eta_2 z$ . We assume that this holds within a box

$$B = \{(x, y, z) \mid -1 \leq x \leq 1, -\frac{1}{2} \leq y \leq \frac{1}{2}, 0 \leq z \leq 1\}$$

around the origin (see Fig. 2). The maps of interest

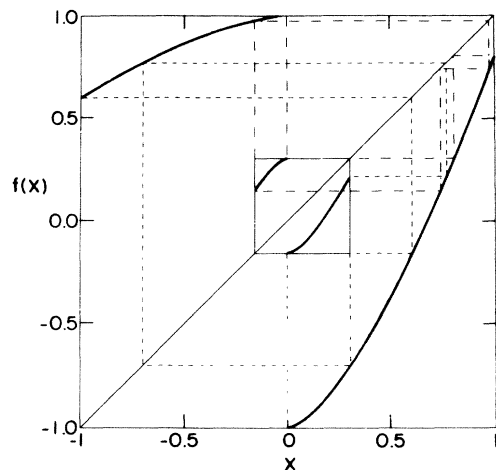


FIG. 1. A graph of the map Eq. (1), for  $\zeta = 1.5$ ,  $\mu = \nu = 1$ ,  $a = 0.3978\dots$ ,  $b = 1.8050\dots$ . The inner box shows the restricted threefold-iterated map. Rescaling yields the renormalized map. Equation (6) can be read off by following the dashed lines.

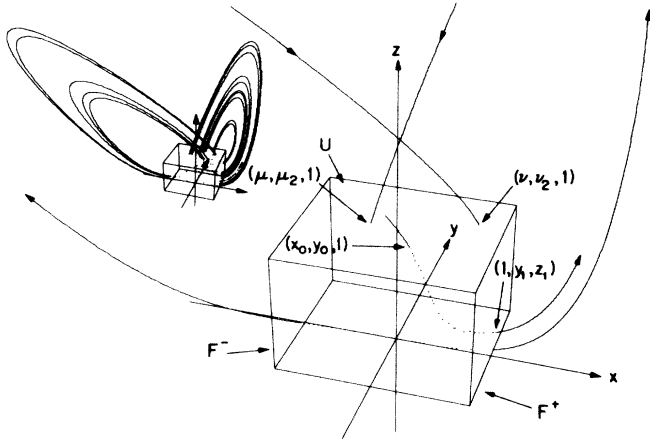


FIG. 2. The box within which the flow is linearized. The inset shows the global structure of the flow.

are return maps on  $U$  (the face  $z=1$  of  $B$ ). Suppose, therefore, that we start at time  $t=0$  at a point  $(x_0, y_0, 1)$  on  $U$ . If  $x_0 > 0$ , its orbit hits the face  $F^+$  of  $B$  at time  $t^* = -(1/\eta_1)\ln x_0$  [i.e.,  $x(t^*) = x_0 e^{\eta_1 t^*} = 1$ ]. Accordingly,

$$(x_0, y_0, 1) \rightarrow (1, y_0 x_0^{\eta_3/\eta_1}, x_0^{\eta_2/\eta_1}) \tag{2}$$

in time  $t^*$ . We thus see that the flow within  $B$  maps any line  $x=\text{const}$  on  $U$  into a line  $z=\text{const}$  on  $F^+$ . The basic assumptions about the global properties of the flow outside the box  $B$  are that lines  $z=\text{const}$  on  $F^+$  are mapped back to lines  $x=\text{const}$  on  $U$  (preserved strong stable foliation<sup>4</sup>), and that the resulting return map from  $U$  to itself is contracting in the  $y$  direction (see Fig. 2). (Needless to say, in general one does not need the original coordinates to be preserved by the flow; any contracting preserved foliation will do.)

Denote now the points where the unstable manifold of the origin hits  $U$  for the first time as  $(-\mu, \mu_2, \mu_3)$  and  $(\nu, \nu_2, \nu_3)$  (see Fig. 2). The assumption on the preserved linear foliation and Eq. (2) (together with its analog for  $x_0 < 0$ ) lead to return maps

$$\begin{pmatrix} x_0 \\ y_0 \\ 1 \end{pmatrix} \rightarrow \begin{pmatrix} -\mu + b x_0^{\eta_2/\eta_1} + \text{h.o.t.}(x_0) \\ \mu_2 + b_2 y_0 x_0^{\eta_3/\eta_1} + \text{h.o.t.}(x_0, y_0) \\ 1 \end{pmatrix}, \tag{3}$$

when  $x_0 > 0$ , and to

$$\begin{pmatrix} x_0 \\ y_0 \\ 1 \end{pmatrix} \rightarrow \begin{pmatrix} \nu - \alpha x_0^{\eta_2/\eta_1} + \text{h.o.t.}(x_0) \\ \nu_2 + \alpha_2 y_0 x_0^{\eta_3/\eta_1} + \text{h.o.t.}(x_0, y_0) \\ 1 \end{pmatrix}, \tag{4}$$

when  $x_0 < 0$ . We thus see that the decoupling of  $x$

from  $y$  and  $z$  allows us to represent the dynamics safely by maps of Eq. (1), with  $\zeta = \eta_2/\eta_1$ . We should stress that the original Lorenz model in its chaotic regime appears to have  $\zeta < 1$ , which leads to cusped return maps favoring first-order transitions to chaos. Therefore, we will focus here on the cases where  $\zeta > 1$ , a condition easily realized with similar flows as we demonstrate below.

To see the richness of dynamical behavior we pick the two-parameter family

$$g_{\mu, \nu}(x) = \begin{cases} \nu - x^2, & x \leq 0, \\ -\mu + x^2, & x > 0, \end{cases} \tag{5}$$

from  $[-\mu, \nu]$  to itself. We should stress that  $\zeta = 2$  is not special here, and (5) is chosen only for concreteness of the forthcoming discussion. The condition  $\mu = \nu$  which yields antisymmetric maps equivalent to unimodal ones is referred to as the ‘‘first diagonal.’’ The condition  $\nu - \nu^2 = \mu^2 - \mu$  which yields continuous circle maps is referred to as the ‘‘second diagonal.’’ We can show<sup>6</sup> that these maps have a unique winding number for values of  $\mu, \nu$  in the  $(\mu, \nu)$  plane which lie below and on the second diagonal. Consequently, this region of  $\mu, \nu$  is naturally partitioned according to the winding number, with irrational winding numbers lying on lines [cf. the partition of the  $(K, \omega)$  plane of the more familiar sine-circle map  $x' = x + \omega - (K/2\pi)\sin(2\pi x) \pmod{1}$  for values of  $K < 1$ ]. Above the second diagonal one can lose the uniqueness of the winding number, but one can always define a rotation interval  $R(g_{\mu, \nu})$ .<sup>6-8</sup>

In analogy to continuous circle maps we define Arnol'd tongues  $\mathcal{A}_w$  and frequency-locked regions<sup>9</sup>  $\mathcal{L}_w$  such that  $\mu, \nu \in \mathcal{A}_w$  if and only if  $R(f_{\mu, \nu}) \in w$  and such that  $\mu, \nu \in \mathcal{L}_w$  if and only if  $R(f_{\mu, \nu}) \equiv \{w\}$ . The part of  $\mathcal{L}_w$  below the second diagonal we call  $\mathcal{M}_w$ . (If  $w$  is irrational we have  $\mathcal{M}_w = \mathcal{L}_w$ .) A sketch of these regions is shown in Fig. 3(a). In the rational case we distinguish in addition another subregion  $\mathcal{R}_{p/q}$  of  $\mathcal{L}_{p/q}$  where  $(f_{\mu, \nu})^q$  restricted to a properly chosen subinterval has again the form (1).

As a consequence the global features of the phase diagram sketched in Fig. 3(b) repeat themselves in each  $\mathcal{R}_{p/q}$ , yielding inductively a hierarchical structure. At each level of this hierarchy, going from  $\mathcal{L}_w$  to the rest of  $\mathcal{A}_w$  when  $w$  is irrational or leaving  $\mathcal{L}_{p/q}$  from the region which is neither in  $\mathcal{M}_{p/q}$  nor in  $\mathcal{R}_{p/q}$  is tantamount to a transition to chaos. Analogous transitions can also be found in continuous circle maps.<sup>10</sup>

There are, however, new codimension-2 scenarios<sup>11</sup> generated by following paths from  $\mathcal{L}_{p/q}$  to  $\mathcal{R}_{p/q}$  at each level of the hierarchy. Such a step is referred to as  $M(p/q \rightarrow w)$  to indicate in which locking one enters at the next level of the hierarchy. The generic

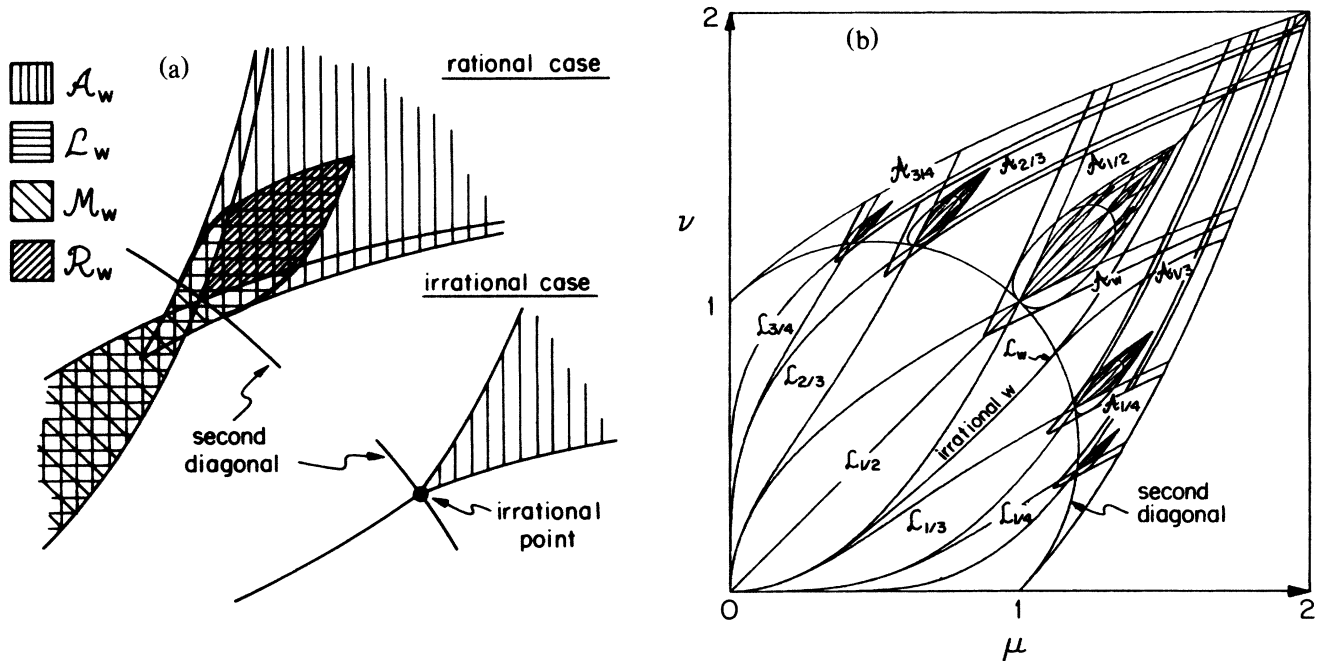


FIG. 3. (a) Blowup of Arnol'd tongues  $\mathcal{A}_w$  near the second diagonal for a rational and an irrational  $w$ . The crosshatched areas indicate the regions mentioned in the text. The bold lines and the irrational points on the second diagonal belong to the boundary of chaos. In this Letter we are concerned with transitions from  $\mathcal{R}_w$  to  $\mathcal{M}_w$ . (b) Sketch of the global structure of the  $\mu$ - $\nu$  phase diagram. Below the second diagonal the plane is partitioned according to the winding number. Above the second diagonal mode-locked regions  $\mathcal{L}_{p/q}$  still exist. In each  $\mathcal{R}_{p/q}$ ,  $q$ -fold iterates of the map, restricted to a proper subinterval, exhibit a similar phase diagram on a reduced scale, etc. *ad infinitum*.

path of this kind will therefore be characterized by

$$M(p_1/q_1 \rightarrow p_2/q_2)M(p_2/q_2 \rightarrow p_3/q_3)M(p_3/q_3 \rightarrow p_4/q_4) \dots$$

corresponding to successive  $q_2, q_3, q_4, \dots$ -furbations. The simplest ones correspond to cases where  $p_n/q_n$  does not depend on  $n$ . These are the ones which will yield a fixed point under renormalization.

To show what kind of universal results appear in these new scenarios we focus (somewhat arbitrarily) on the process of period tripling with  $p_n/q_n \equiv \frac{2}{3}$ . We consider then maps as in Eq. (1) and Fig. 1, and look for a functional renormalization-group theory for this period tripling. One can show (cf. Fig. 1) that the relevant functional equations for this problem of tripling in this space of functions are

$$\begin{aligned} f'_R(x) &= \alpha f_R \circ f_L \circ f_R(x/\alpha), \\ f'_L(x) &= \alpha f_R \circ f_R \circ f_L(x/\alpha). \end{aligned} \tag{6}$$

Since  $\zeta = \eta_2/\eta_1$ , in the original flow, values of  $\zeta$  close to 1, i.e.,  $\zeta = 1 + \epsilon$ , represent real and interesting problems. Consequently, solving Eqs. (6) by methods of  $\epsilon$  expansion<sup>12</sup> yields physically relevant predictions. We notice that the pieces of the relevant third iterates of the map (before rescaling) appear in the box formed by the interval

$$[-\mu + a(\nu - b\mu^\zeta)^\zeta, -\mu + a(-\mu + a\nu^\zeta)^\zeta].$$

Accordingly, the rescaling factor  $\alpha$  is given by

$$\alpha = -\mu / [-\mu + a(\nu - b\mu^\zeta)^\zeta], \tag{7}$$

and (6) is approximated by

$$\frac{-\mu' + a'x^\zeta}{\alpha} = -\mu + a\{\nu - b[-\mu + a(x/\alpha)^\zeta]^\zeta\}^\zeta, \tag{8a}$$

$$\frac{-\mu' - b'x^\zeta}{\alpha} = -\mu + a\{-\mu + a[\nu - b(x/\alpha)^\zeta]^\zeta\}^\zeta. \tag{8b}$$

For  $\zeta = 1$  we find the fixed point  $a^* = b^* = 1$ ,  $\mu^* = 1$ ,  $\nu = 2$ ,  $\alpha = \infty$ .<sup>13</sup> The eigenvalues of the linearized recursion relations are  $\lambda_1 = 0$ ,  $\lambda_2 = 1$ ,  $\lambda_3 = 3$ ,  $\lambda_4 = \infty$ . For  $\zeta = 1 + \epsilon$  we seek solutions of the form  $a = b = 1 + \gamma$ ,  $\nu = 2 + \beta$  and look for the corrections to the relevant eigenvalues  $\lambda_3, \lambda_4$ . Equation (7) leads to

$$\alpha = -1/\beta. \tag{9}$$

Expanding Eqs. (8) to first order we find the fixed-point solutions

$$-\beta^* = \gamma^*, \quad \epsilon = -2\gamma^*/\ln\gamma^*. \tag{10}$$

Linearizing the recursion relations we obtain the two relevant eigenvalues

$$\lambda_3 = 3 - 2/\ln\gamma^*, \quad \lambda_4 = 3/\gamma^*. \quad (11)$$

These predictions can be compared to direct numerical simulations. In the simulations we chose Eqs. (1) with  $\mu = \nu = 1$  leaving  $a$  and  $b$  as parameters for every given  $\zeta$ . We found numerically<sup>7</sup> values of the parameters leading to superstable orbits of order 3, 9, 27, 81, and 243 for various values of  $\zeta$ . The values of parameters  $\mu, \nu$  appear to converge geometrically with a rate  $\delta$  (e.g.,  $\delta = 4.14, 4.51, 6.62, 8.7$  for  $\zeta = 1.05, 1.1, 1.5, 2$ ). The value of  $\delta$  should be compared with  $\lambda_3$  of Eq. (11). For  $\epsilon = 0.05$  the agreement is better than 10% which is satisfactory in view of the large correction obtained to this order. The agreement between the calculated  $\alpha$  values<sup>7</sup> and Eq. (9) is even closer, as usual. Notice that it can be proven that all new scenarios we discuss in this Letter indeed lead to chaos. Furthermore the renormalization group also describes the onset of chaos, yielding for the increase of the topological entropy the same critical exponents as for the  $q$ -fibrations.

Finally we give an example of a flow that seems to realize the conditions and results of the present theory.<sup>5,14</sup>

$$\begin{aligned} \dot{x} &= 1.8(x - y) + \epsilon x^2, & \dot{y} &= -7.2y + xz + \mu x^3, \\ \dot{z} &= -2.7z + xy - 0.07z^2. \end{aligned} \quad (12)$$

The eigenvalues at the origin are  $\eta_1 = 1.8$ ,  $\eta_2 = 2.7$ ,  $\eta_3 = 7.2$ . Thus  $\zeta = 1.5$ . We determined<sup>7</sup> the parameter values where the flow has period  $3^n$  with winding number  $\frac{2}{3}$  for  $n = 1, 2, 3, 4$ . We found  $\delta_{\text{flow}} = 6.66$  which is in excellent agreement with  $\delta_{\text{map}} = 6.62$  for  $\zeta = 1.5$ .

For simplicity we chose  $\zeta$  to be constant. The origin is therefore always unstable. Generically, the spectrum of eigenvalues will depend on the parameters as for example in the case of the Lorenz model. The routes to chaos described above would then follow a transition from a globally attracting fixed point to a pair of stable fixed points and a subsequent pair of supercritical Hopf bifurcations. Since the global picture

described above is robust to small perturbations and since our flow example is certainly not exotic, it appears worthwhile to seek experimental realizations of the scenarios found above.

This work was partially supported by the Minerva Foundation.

<sup>(a)</sup>Permanent address: U.A.168, Parc Valrose, 06034 Nice Cédex, France.

<sup>(b)</sup>Permanent address: Institut für Festkörperforschung der Kernforschungsanlage, D-5170 Jülich, W. Germany.

<sup>(c)</sup>Also at the Hebrew University of Jerusalem and at the Mathematics Department of the Weizmann Institute of Science, Rehovot 76100, Israel. Permanent address: Physique Théorique, Parc Valrose, 06034 Nice Cédex, France.

<sup>1</sup>For a collection of relevant papers see *Chaos*, edited by Hao Bai-Lin (World Scientific, Singapore, 1984).

<sup>2</sup>E. N. Lorenz, *J. Atmos. Sci.* **20**, 130 (1963).

<sup>3</sup>P. Cvitanović and J. Myrheim, *Phys. Lett.* **94A**, 329 (1983).

<sup>4</sup>J. Guckenheimer, in *The Hopf Bifurcation and its Application*, edited by J. E. Marsden and M. McCracken, Applied Mathematical Sciences Vol. 19 (Springer, New York, 1976), p. 368.

<sup>5</sup>A. Arnéodo, P. Coulet, and C. Tresser, *Phys. Lett.* **81A**, 197 (1981).

<sup>6</sup>C. Tresser, *C. R. Acad. Sci., Ser. 1* **296**, 729 (1983); J.-M. Gambaudo and C. Tresser, *C. R. Acad. Sci., Ser. 1* **300**, 311 (1985).

<sup>7</sup>I. Procaccia, S. Thomae, and C. Tresser, to be published.

<sup>8</sup>S. Newhouse, J. Palis, and F. Takens, *Inst. Hautes Etudes Sci. Publ. Math.* **57**, 5 (1983).

<sup>9</sup>R. S. McKay and C. Tresser, *Physica (Amsterdam) D* (to be published).

<sup>10</sup>For a review of all these transitions see Ref. 9 and references therein.

<sup>11</sup>In this space period doubling is also a codimension-2 bifurcation: See P. Collet, P. Coulet, and C. Tresser, *J. Phys. (Paris), Lett.* **46**, L-143 (1986).

<sup>12</sup>B. Derrida, A. Gervois, and Y. Pomeau, *J. Phys. A* **12**, 269 (1979); P. Collet, J.-P. Eckmann, and O. E. Lanford, *Commun. Math. Phys.* **76**, 211 (1980).

<sup>13</sup>One should note that in the case  $\zeta = 1$ , the "second diagonal" coincides with the boundary of chaos: See Ref. 6.

<sup>14</sup>J.-M. Gambaudo, P. A. Glendinning, and C. Tresser, *J. Phys. (Paris) Lett.* **46**, L-653 (1985).